









# MODELING OF PLAQUE FORMATION AND DEVELOPMENT IN ARTREAT AND TAXINOMISIS PROJECTS

Nenad Filipovic<sup>1,2\*</sup>  [0000-0001-9964-5615], Milos Radovic<sup>2</sup>  [0000-0001-5896-0563], Tijana Djukic<sup>2,3</sup>   
[0000-0002-9913-6527], Igor Saveljic<sup>2,3</sup>  [0000-0002-0707-5174], Bogdan Milicevic<sup>2,3</sup>  [0000-0002-0315-8263],  
Exarchos Themis<sup>4</sup>  [0000-0001-9420-9419], Oberdan Parodi<sup>5</sup>  [0000-0003-2459-1047], Dimitris Fotiadis<sup>4</sup>  
 [0000-0002-3258-9441]

<sup>1</sup> Faculty of Engineering, University of Kragujevac, Kragujevac, Serbia

e-mail: fica@kg.ac.rs

<sup>2</sup> Bioengineering R&D Center, BioIRC, Serbia

<sup>3</sup> Institute for information technology Kragujevac, University of Kragujevac, Serbia

<sup>4</sup> University of Ioannina, Ioannina, Greece

<sup>5</sup> National Research Council Pisa, Italy

*\*corresponding author*

## Abstract

This review summarizes scientific findings from three European Commission FP7 projects. The first, ARTREAT (2008-2013), focused on a multi-level, patient-specific model of artery and atherogenesis for outcome prediction, treatment decision support, and virtual hands-on training. An original method for plaque formation and development was created and validated using pilot study patients with coronary and carotid artery disease in EU clinical centers. Additionally, results from the TAXINOMISIS project (2018-2024) are discussed. This project aimed to develop a multidisciplinary approach to stratify patients with carotid artery disease, employing continuum and Agent-Based Modeling (ABM) techniques to study plaque progression. The goal was to create an innovative, multiscale risk stratification model that integrates clinical and personalized data, plaque and brain imaging, computational modeling, and novel biomarkers to distinguish high-risk from low-risk patients. Researchers from University of Kragujevac and BioIRC participated in this project with colleagues from European Union.

**Keywords:** atherosclerosis, plaque formation, computer modeling, ABM, coronary and carotid artery.

## 1. Introduction

### 1.1 Atherosclerosis model in the coronary artery

Atherosclerosis is a progressive condition characterized by the buildup of lipids and fibrous tissue in large arteries, with current understanding highlighting the importance of the biological features of atheroma for its clinical implications (Libby et al., 2002). The inflammatory process begins when low-density lipoproteins (LDL) penetrate the arterial intima, triggering leukocyte recruitment. Vascular cell adhesion molecule-1 (VCAM-1) plays a key role in the adhesion of

mononuclear leukocytes at early atheroma sites (Kaazempur-Mofrad and Ethier, 2001). This interaction leads to the formation of fatty streaks, which are the initial lesions of atherosclerosis and can develop into more complex plaques. The ARTREAT project conducted a computational study to model LDL transport concerning macrophages and oxidized LDL distribution, focusing on early plaque growth within the intima. The study utilized the Navier-Stokes equations to simulate blood flow in the lumen, Darcy's law for blood filtration, Kedem-Katchalsky equations (Kedem and Katchalsky, 1958, 1961) for solute exchange, and a system of reaction-diffusion equations to depict the inflammatory response and lesion development. Assuming matter incompressibility, the project provided simulation examples of plaque formation and progression (Filipovic et al., 2012, 2013).

### *1.2 Agent based model of atherosclerosis*

The complexity of atherosclerosis involves various components that contribute to plaque formation and growth, each with distinct characteristics, behaviors, and rules. The interaction between these components and their environment determines the progression of the plaque. To effectively model this process, we selected the Agent-Based Model (ABM) approach, which simulates the behaviors of individual agents to reproduce plaque evolution and arterial remodeling. This dynamic system allows complex phenomena to emerge from simple, rule-based interactions among agents within a continuously changing environment. ABMs are valuable tools for uncovering intricate causal relationships and underlying mechanisms, especially in systems characterized by numerous agents that collect information, learn, and act simultaneously within a nonlinear, spatiotemporal context (Chan, 2001). Each agent follows specific decision rules, and their collective actions over time give rise to emergent phenomena. This bottom-up approach emphasizes the importance of individual behaviors and local interactions, which lead to higher-level system patterns without requiring detailed prediction of the entire system. ABMs also offer significant flexibility in modeling heterogeneity among agents, in attributes, behaviors, and mobility, making them well-suited for capturing complex individual dynamics that subsequently influence system-wide outcomes (Bonabeau, 2002). Furthermore, ABMs provide a cost-effective and efficient alternative to physical experiments, enabling exploration of different scenarios and decision-making strategies in a virtual environment—allowing researchers to evaluate potential outcomes before implementing real-world interventions (Bazghandi, 2012).

When the responses of complex biological systems depend on multicellular behavior influenced by microenvironmental changes, multi-scale modeling becomes essential. Techniques such as cellular automata (CA) and ABM are employed to analyze cardiovascular tissues and regulatory processes (Zahedmanesh, Cahill, & Lally, 2012). For example, Pappalardo et al. developed a 2D agent-based model to simulate early-stage atherosclerosis and immune responses, incorporating key cellular entities and their interactions that drive atherogenesis (Pappalardo, Musumeci, & Motta, 2008). Further studies examined whether short-term high LDL levels could cause irreversible damage and whether lowering LDL might reduce atherosclerosis risk (Pappalardo, Cincotti, Motta, & Pennisi, 2009). Similarly, Curtin and Zhou designed a 2D ABM to simulate restenosis after angioplasty and stent placement, exploring how different vessel geometries and stent designs influence restenosis development (Curtin & Zhou, 2014). Olivares et al. extended this research with a 3D ABM focusing on cellular and molecular mechanisms involved in foam cell formation, emphasizing LDL oxidation and macrophage transformation (Olivares, Gonzales Ballester, & Noailly, 2016).

Beyond discrete methods, hybrid numerical techniques such as the Finite Element Method (FEM) can provide a comprehensive framework, particularly for analyzing arterial wall stresses and their role in atherogenesis. This includes assessing wall shear stress (WSS) and its effect on endothelial cell behavior, permeability to LDL, and the dynamics of smooth muscle cells

(SMCs) and the extracellular matrix (ECM) (Chatzizisis et al., 2007). Zahedmanesh and Lally combined 2D ABM with FEM to model vascular damage—FEM quantified stresses related to stent deployment, while ABM simulated cellular migration, proliferation, and ECM response to injury. This hybrid approach was successfully applied to model vascularization in tissue-engineered blood vessels, providing insights into how scaffold properties influence smooth muscle cell growth and hyperplasia (Zahedmanesh & Lally, 2012).

Additionally, Garbey et al. developed a hybrid model integrating Partial Differential Equations (PDE) and ABM to simulate vascular adaptation after interventions, effectively capturing hemodynamic forces while tracking cell behaviors such as proliferation, apoptosis, and ECM production (Garbey, Rahman, & Berceci, 2015). Later enhancements improved the model's ability to simulate cellular movement and behavior across membranes (Garbey, Casarin, & Berceci, 2019). These multiscale models of atherosclerosis successfully depict the interplay between hemodynamics and arterial wall remodeling during plaque development, incorporating stochastic cellular dynamics with blood flow simulations for a comprehensive understanding of the process (Bhui & Hayenga, 2017; Corti et al., 2019, 2020).

In this review we have presented results of TAXINOMISIS (<https://taxinomisis-project.eu/>) project.

## 2. Materials and methods

### 2.1 Modeling of plaque formation and progression

Mass transfer problem for LDL transport through the wall and then a continuum based approach for plaque formation and development in three-dimension is firstly described. The governing equations and numerical procedures are given. The three-dimensional Navier-Stokes equations, together with the continuity equation are used for blood flow numerical modeling

$$-\mu \nabla^2 u_l + \rho (u_l \cdot \nabla) u_l + \nabla p_l = 0 \quad (1)$$

$$\nabla u_l = 0 \quad (2)$$

where  $u_l$  is blood velocity in the lumen,  $p_l$  is the pressure,  $\mu$  is the dynamic viscosity of the blood, and  $\rho$  is the density of the blood.

Mass transfer in the blood lumen is coupled with the blood flow and modeled by the convection-diffusion equation as follows

$$\nabla \cdot (-D_l \nabla c_l + c_l u_l) = 0 \quad (3)$$

in the fluid domain, where  $c_l$  is the solute concentration in the blood domain, and  $D_l$  is the solute diffusivity in the lumen (Kojic et al 2008, Kojic et al 1998).

Mass transfer in the arterial wall is coupled with the transmural flow and modeled by the convection-diffusion-reaction equation as follows

$$\nabla \cdot (-D_w \nabla c_w + k c_w u_w) = r_w c_w \quad (4)$$

in the wall domain, where  $c_w$  is the solute concentration in the arterial wall,  $D_w$  is the solute diffusivity in the arterial wall,  $k$  is the solute lag coefficient, and  $r_w$  is the consumption rate

constant. LDL transport in lumen of the vessel is coupled with Kedem-Katchalsky equations (Kedem and Katchalsky, 1958, 1961):

$$J_v = L_p (\Delta p - \sigma_d \Delta \pi) \quad (5)$$

$$J_s = P \Delta c + (1 - \sigma_f) J_v \bar{c} \quad (6)$$

where  $J_v$  is the transmural velocity,  $J_s$  is the solute flux,  $L_p$  is the hydraulic conductivity of the endothelium,  $\Delta c$  is the solute concentration difference across the endothelium,  $\Delta p$  is the pressure drop across the endothelium,  $\Delta \pi$  is the oncotic pressure difference across the endothelium,  $\sigma_d$  is the osmotic reflection coefficient,  $\sigma_f$  is the solvent reflection coefficient,  $P$  is the solute endothelial permeability, and  $\bar{c}$  is the mean endothelial concentration.

We used a single layer model while multilayered model is still developing. The first term in Kedem-Katchalsky equations  $P \Delta c$  of the right hand side in (Eq 6) defines the diffusive flux across the endothelium, while the second term  $(1 - \sigma_f) J_v \bar{c}$  defines the convective flux. Here we do not neglect the convective term. Only the oncotic pressure difference  $\Delta \pi$  is neglected because of decoupling the fluid dynamics from solute dynamics. Incremental-iterative procedure to treat the convective diffusion terms for LDL transport have been used.

The inflammatory process was solved using three additional reaction-diffusion partial differential equations (Filipovic et al 2012, 2013):

$$\begin{aligned} \partial_t O_x &= d_1 \Delta O_x - k_1 O_x \cdot M \\ \partial_t M + \text{div}(v_w M) &= d_2 \Delta M - k_1 O_x \cdot M + S / (1 + S) \\ \partial_t S &= d_3 \Delta S - \lambda S + k_1 O_x \cdot M + \gamma (O_x - O_x^{thr}) \end{aligned} \quad (7)$$

where  $O_x$  is the oxidized LDL or  $c_w$  - the solute concentration in the wall from eq. (4);  $M$  and  $S$  are concentrations in the intima of macrophages and cytokines, respectively;  $d_1, d_2, d_3$  are the corresponding diffusion coefficients;  $\lambda$  and  $\gamma$  are degradation and LDL oxidized detection coefficients; and  $v_w$  is the inflammatory velocity of plaque growth, which satisfies Darcy's law and continuity equation (Filipovic et al 2006, 2012, 2013):

$$v_w - \nabla \cdot (p_w) = 0 \quad (8)$$

$$\nabla v_w = 0 \quad (9)$$

in the wall domain. Here,  $p_w$  is the pressure in the arterial wall.

## 2.2 Agent-Based Modeling

We employed a methodology based on Corti et al. (Corti et al., 2020), which involves four iterative steps (see Fig. 1). The process is summarized as follows: 1) preparation of the geometry, 2) CFD simulation, 3) ABM simulation, and 4) creation of a new 3D geometry. During the geometry preparation phase, a 3D model of a healthy artery is constructed, and a 3D mesh of the fluid domain is generated using PAK software. To analyze hemodynamics and extract wall shear stress (WSS) values at the lumen interface of cross-sectional slices, CFD simulations are performed within PAK. For each cross-section, we then simulate hemodynamic-

driven remodeling by integrating ABM, which models cellular, extracellular, and lipid dynamics. CFD provides the WSS values, while ABM is utilized to simulate arterial wall remodeling based on these hemodynamic forces.

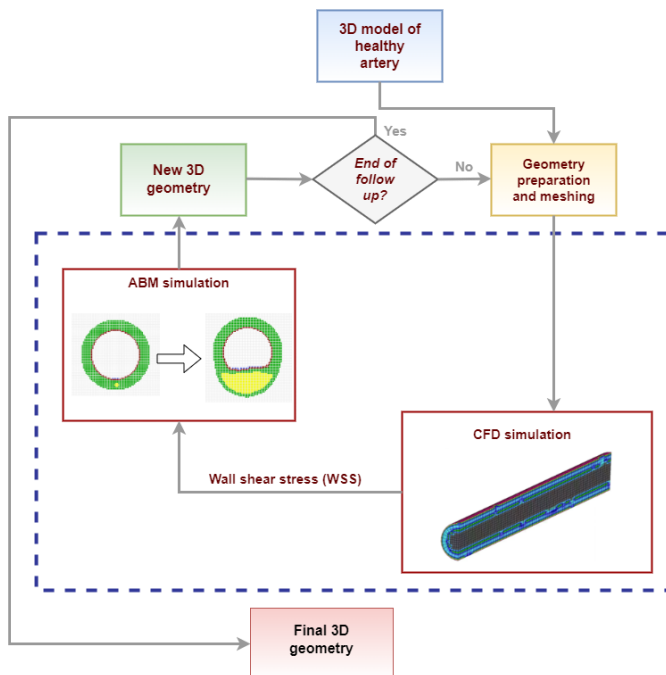


**Fig. 1.** Workflow of the proposed framework

In each 2D cross-section, all geometric changes modeled by the ABM were transferred to the fluid domain, enabling blood flow calculation and the subsequent determination of WSS for the next iteration of the process. Each geometric modification in the 2D cross-sections influences the fluid dynamics, so the ABM module is coupled with the CFD module to ensure that the WSS distribution is continuously updated. The ABM simulates arterial wall remodeling by modeling cellular processes such as mitosis, ECM production and degradation, and lipid infiltration into the intima. Additionally, various vessel structures, compositions, and cellular events were incorporated into this work, based on the ABM developed by Corti et al. (2020). The behavior of the ABM was validated under atherogenic conditions. The CFD-ABM coupling used hemodynamic data to initialize the ABM, which was conducted in a 2D circular cross-section comprising three concentric layers: tunica intima, media, and adventitia. Figure 3a illustrates this cross-section, including the cellular and ECM compositions of each layer. Figure 3b shows the Internal Elastic Lamina (IEL) and External Elastic Lamina (EEL), while Figure 3c presents the cellular makeup, including Smooth Muscle Cells (SMCs) in the intima and media and fibroblasts in the adventitia. Finally, Figure 2 displays the ECM components, such as elastin and collagen in the intima and media, and collagen in the adventitia.

The 2D ABM is fed with an initial WSS profile (Bentzon, Otsuka, Virmani, & Falk, 2014; Chatzizisis, et al., 2007). Also, low WSS affects endothelial function by reducing atheroprotective genes and increasing the atherogenic ones, which leads to atherosclerotic plaque formation (Cheng, et al., 2004).

WSS values were obtained from the 3D CFD simulation. A level of endothelial dysfunction  $D^i$  was computed as given in (5.1).  $WSS^i$  is the WSS at site  $i$  and  $WSS_o = 1 Pa$  is the WSS threshold.

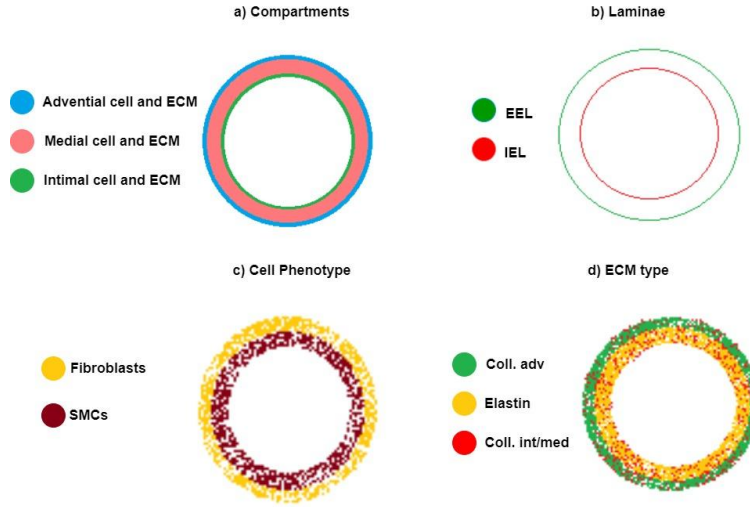


**Fig. 2.** Initialization of agent based model

$$D(WSS)^i = D^i = \begin{cases} (1 - \frac{WSS^i}{WSS_o}), & \text{if } WSS^i < WSS_o \\ 0, & \text{otherwise} \end{cases} \quad (10)$$

$WSS_o$  was set following the study by (Samady, et al., 2011). Each dysfunctional endothelial site  $i$ , with  $D^i \neq 0$ , starting a state of alteration that diffuses within the intima through isotropic diffusion, from a peak of intensity  $D^i$  with a diffusion constant  $\varphi$ .  $A^{(i,k)}(D^i, d)$  is the level of alteration produced by the  $i$ -th endothelial site and recorded at the  $k$ -th site within intima, at a distance  $d$  from  $i$  (11).

$$A^{(i,k)}(D^i, d) = A^{(i,k)} = D^i * e^{-\frac{1}{2} \left( \frac{d}{4\varphi t} \right)^2} \quad (11)$$

For each site  $k$ , the individual states of alteration are summed up to define the global level of inflammation of the  $k$ -th site  $I^k$  in (12).  $N_L$  is the initial number of sites of the lumen wall and the resulting  $I^k$  affects the agent dynamics,

$$I^k = \sum_{i=1}^{N_L} A^{(i,k)} \quad (12)$$

If all the WSS values at the  $i$ -th sites are larger than the threshold,  $D^i = 0 \forall i$  and  $I^k = 0$  everywhere. If  $WSS^i < WSS_0$ , a state of inflammation  $I$  develops and the mechanisms of plaque formation are activated. Then, related WSS profile was defined as atherogenic.

The baseline densities of probability were set for cell mitosis/apoptosis and ECM deposition/degradation to replicate the physiologic conditions. They were defined with Eq. (13) and Eq. (14), respectively:

$$p_{mit} = p_{apop} = \alpha_1 \quad (13)$$

$$p_{prod} = \beta * p_{deg} = \alpha_4 \quad (14)$$

where  $\alpha_1$ ,  $\alpha_4$  and  $\beta$  were involved in order to maintain the physiological cell/ECM ratio which is defined for each tissue layer during the phase of initialization. (Garbey, Casarin, & Berceci, 2017).

Considering the work of Garbey et al. (Garbey, Casarin, & Berceci, 2017), coefficient  $\beta$  for the intima, media and adventitia layers were set in order to guarantee stable trends of ECM in each layer under baseline conditions. With the specified calibrated coefficients, Eq. (13) and Eq. (14) trigger physiological remodeling of the wall, leading to the replication of the homeostatic state of a healthy artery. The probability of cell mitosis and ECM production in the intima increases with the inflammation level which directly cause the number of neighboring lipids and the closeness to the lumen (Doran, Meller, & McNamara, 2008), leading to the following:

$$p_{mit} = \begin{cases} \alpha_1 \cdot (1 + \alpha_2 I^k) & \text{if } n_{lip} = 0 \\ \alpha_1 \cdot (1 + \alpha_2 I^k) (1 + \alpha_3 n_{lip}) \left\{ 1 + \exp(-d_{lumen}^k) \right\} & \text{if } n_{lip} \neq 0 \end{cases} \quad (15)$$

$$p_{prod} = \begin{cases} \alpha_4 \cdot (1 + \alpha_2 I^k) & \text{if } n_{lip} = 0 \\ \alpha_4 \cdot (1 + \alpha_2 I^k) (1 + \alpha_3 n_{lip}) \left\{ 1 + \exp(-d_{lumen}^k) \right\} & \text{if } n_{lip} \neq 0 \end{cases} \quad (16)$$

where  $\alpha_2$  and  $\alpha_3$  weight the effect of the inflammation state  $I^k$  and the influence of the neighboring lipids  $n_{lip}$ , while  $d_{lumen}^k$  is the distance between the site  $k$  and the lumen wall. The coefficients were set following the framework proposed by Corti et al. (Corti, et al., 2020).

Lipid dynamics is activated once the intima thickens over a given threshold (Bentzon, Otsuka, Virmani, & Falk, 2014). The probability of lipid infiltration is computed as the probability of a site  $k$  expressed by:

$$p_{lipid} = \alpha_5 \cdot (1 + I^k) \left\{ 1 + \alpha_6 \cdot \exp(-d_{lip}^k) \right\} \left( 1 + \frac{n_{lip}}{\alpha_7} \right) \quad (17)$$

where  $\alpha_5$  sets the event probability in the interval (0, 1). The terms  $\alpha_6 \cdot \exp(-d_{lip}^k)$  and  $\left( 1 + \frac{n_{lip}}{\alpha_7} \right)$  promote lipid clustering, by increasing the probability of a lipid to occupy a site  $k$  close to another lipid, whose distance is  $d_{lip}^k$ . At each time step, only one lipid molecule can

penetrate the intima. The parameters and coefficients in Eq. (17) are configured to produce a lipid nucleus that aligns with histological characteristics (Otsuka et al., 2013). When lipids enter the intima, they must remain stationary throughout the entire simulation. Therefore, their movement is restricted to the shortest path that avoids passing through other lipid agents, ensuring the stability of the lipid core. All agent movements are guided by the principle of minimizing energy, except in the specific case where lipid agents are positioned along the shortest path, in which they remain fixed.

A unique 3D geometry of the lumen vessel is built and starting ABM configuration of each plane for the following cycle will be determined. Specifically, for each ABM solution of a given cross-section  $M$ , lumen and external radius, as well as plaque thickness, were computed and indicated as  $R_j^i(\vartheta)$ , with  $j=1,2,3$ , respectively. The corresponding deviation,  $\Delta^i$ , from the average configuration  $\overline{R_j^i(\vartheta)}$ , was computed as defined in Eq. (18), and the ABM  $i$ -th output minimizing  $\Delta$  was selected:

$$\Delta^i = \sum_{j=1}^3 \int_0^{2\pi} w_j \sqrt{\left(R_j^i(\vartheta) - \overline{R_j^i(\vartheta)}\right)^2} dV \quad (18)$$

where each  $j$ -th quantity is weighed by  $w_j$ . The same criterion was applied for all cross-sections and the 3D geometry was finally reconstructed.

### 3. Results

#### 3.1 Results for ARTREAT project for coronary artery

In the clinical study during ARTREAT project (2008-2013) we examined plaque position for the coronary artery for baseline and follow-up time. Stent position are also included in patients. Measurements are done with CT and the results are compared with numerical modeling.

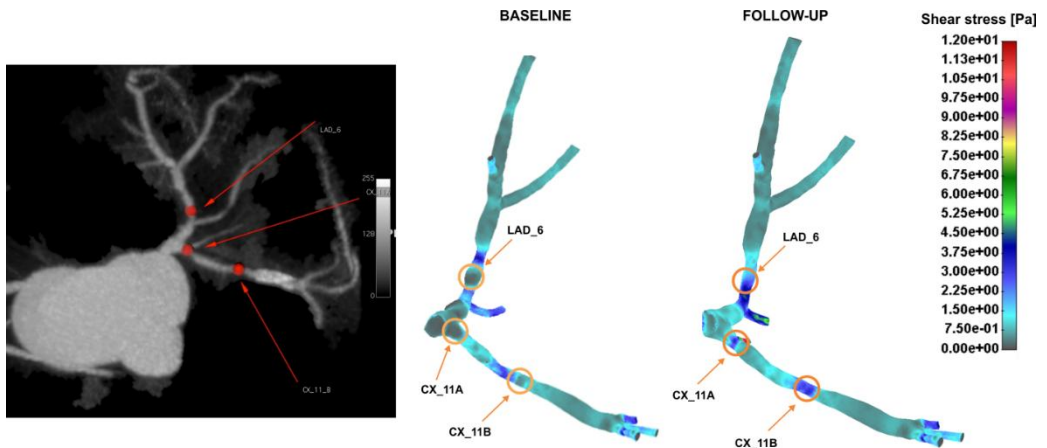


**Fig. 3.** Baseline and follow-up for plaque position at CX and LAD

Plaque position at CX and LAD artery for baseline and follow-up is presented in Fig. 3. Stent position also can be seen from the Fig. 4. Shear stress and plaque concentration for this patient



has been shown in Fig. 4. It can be seen that plaque concentration on the specific cross-section location is matched with CT measurement.

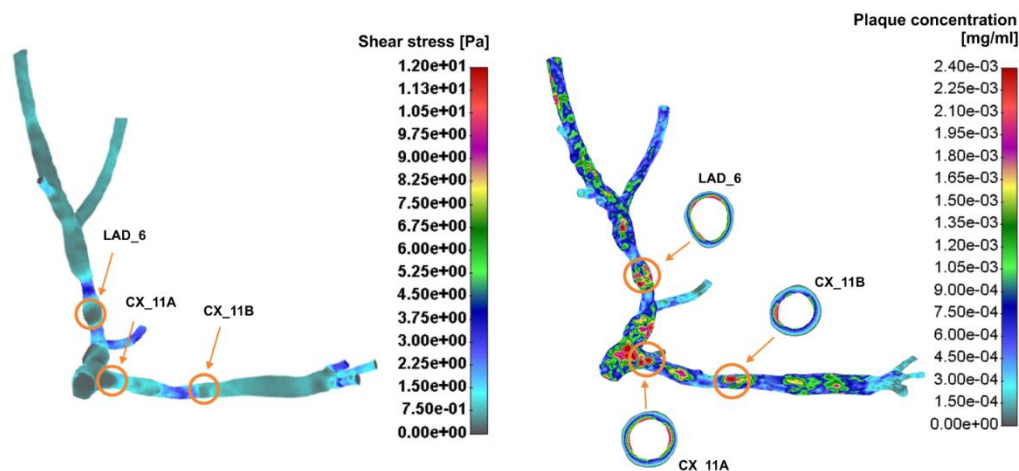


**Fig. 4.** Shear stress and plaque concentration for coronary artery patient

### 3.2 Results for ARTREAT project for carotid artery

We analyzed changes in the cross-sectional areas of the carotid artery in different patients to study disease progression. Out of 50 patients, we selected two exhibiting significant MR plaque progression to estimate parameters for our plaque formation and development model. From MR images, we segmented the inner and outer walls at nine cross-sections at baseline, three months, and twelve months. Segmented data for patient #1 are shown in Fig. 5a. The trends of increasing or decreasing cross-sectional areas over time for this patient are illustrated in Fig. 5b, which indicates that nearly all areas tend to increase during follow-up. For the same patient, the relationship between cross-sectional area changes and wall shear stress (WSS) zones is depicted in Fig. 5c. Three color categories were used: red indicates large decreases in cross-sectional area with moderate WSS, yellow indicates small decreases in area with moderate WSS, and green represents increases in area associated with low WSS. From Fig. 5c, it is evident that there is a significant correlation between large increases in cross-sectional areas and regions of low wall shear stress for patient #1.

### 3.3 TAXINOMISIS project, example of patient-specific carotid artery

The atherosclerotic progression within the 3D models of carotid arteries (**NKUA dataset**) was simulated using PAK Athero and PAK ABM approach. The results are presented at the follow up 1 and follow up 3 in order to compare disease progression. The fluid and solid domains were separated. Also, wall domain included separated plaque area. In wall domain the ABM was used as 8 agents inside each finite element. The results for four NKUA patients reconstructed based on MRI imaging data are presented comparing PAK Athero and PAK ABM for follow up 1 and follow up 3, while results for each patient present oxidized LDL (Fig. 6). The ABM model was used with convergence  $1e^{-5}$  per time step. The time domain was simulated with increased flux for follow up 1 and follow up 3.

It can be seen that oxidized LDL in PAK ABM model is a little higher then in PAK Athero model. That is probably because ABM functions (15) and (16) give higher values for the same shear stress and agent movements are stronger then continuum level of calculation which was implement in PAK Athero model. Lipid dynamics described in Eq. (17) is also faster than continuum approach which gives more realistic scenario of plaque growing due to interaction of the different agents moving and relation between them.

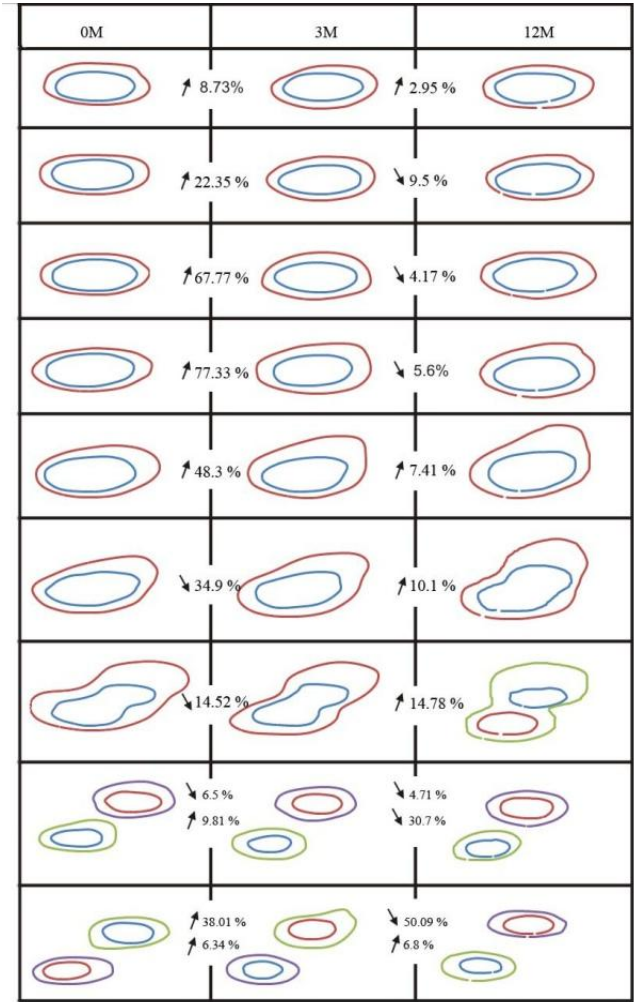


**Fig. 5a.** Cross-section areas changes for patient #1 (area between the inner and the outer wall)

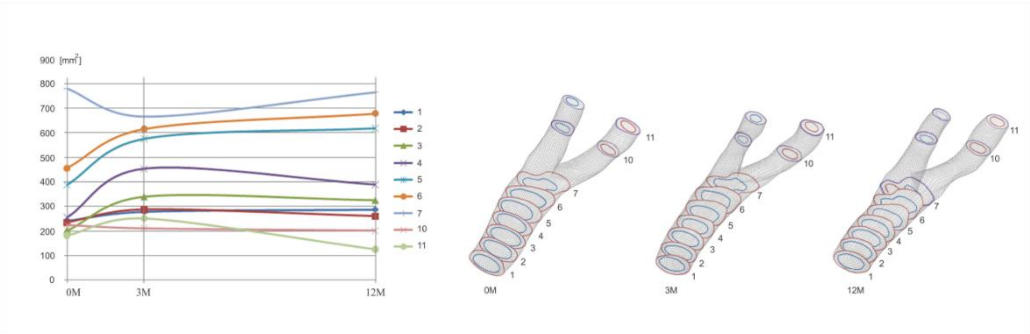


Fig. 5b. Cross-section areas vs time (0, 3 and 12 months) for patient #1

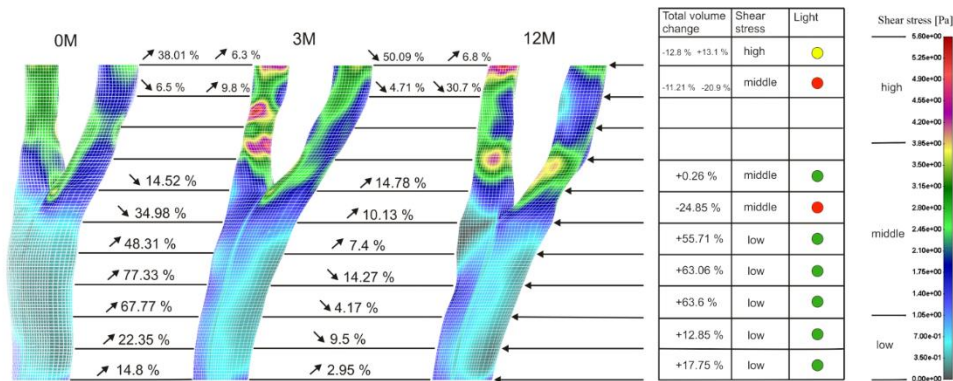
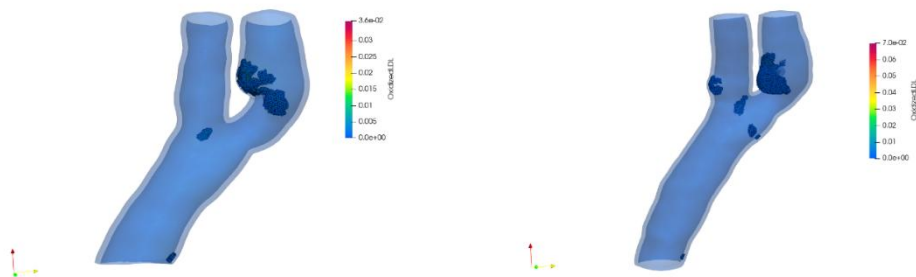
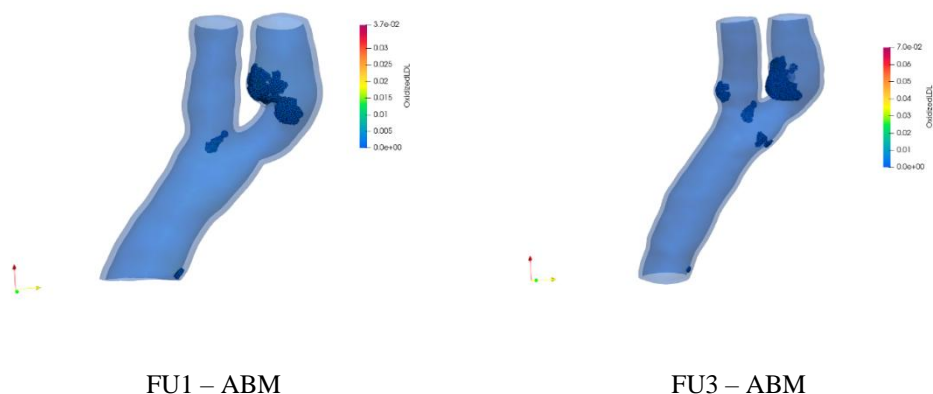


Fig. 5c. Correlation of cross-sections changes with wall shear stress for patient #1



FU1 – Athero21

FU3 – Athero21



**Fig. 6.** NKUA#04 MRI - Simulated plaque progression using PAK Athero21 and PAK ABM at follow up 1 and follow up 3

In the Fig. 7 we presented results for PAK ABM results at follow up 1 and follow up 3 where different color points represent different materials. For example, blue color is lumen domain, grey color is wall and red color is plaque. During process of plaque growing different points are changing color from grey or blue to red color which directly denotes plaque growing.

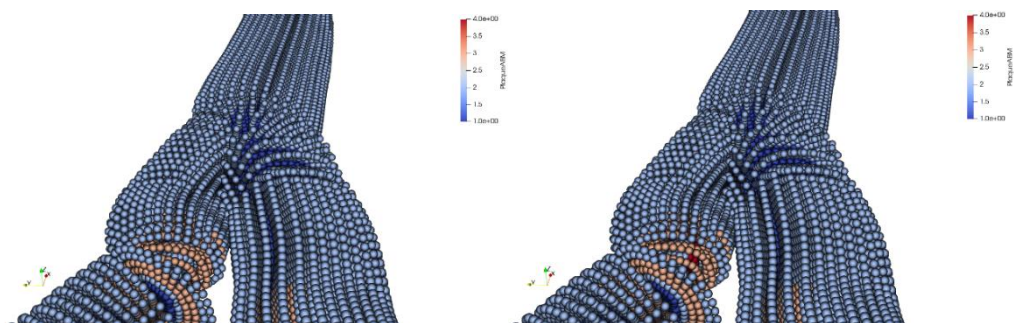


**Fig. 7.** Patient NKUA#51 US, results for PAK ABM at follow up 1 and follow up 3, different color points represent different materials.

Similar results have been produced for other patients. In PAK ABM solver we can see plaque growing with different change of color for materials. In this way we can calculate volume size for plaque during time. The following Figures (7-11) present plaque results (follow-up 1 and follow-up 3) obtained with PAK ABM for NKUA patients #4, #6 and #25. The cutting planes are included, enabling better insight in carotid branche (ICA) under atherosclerosis.

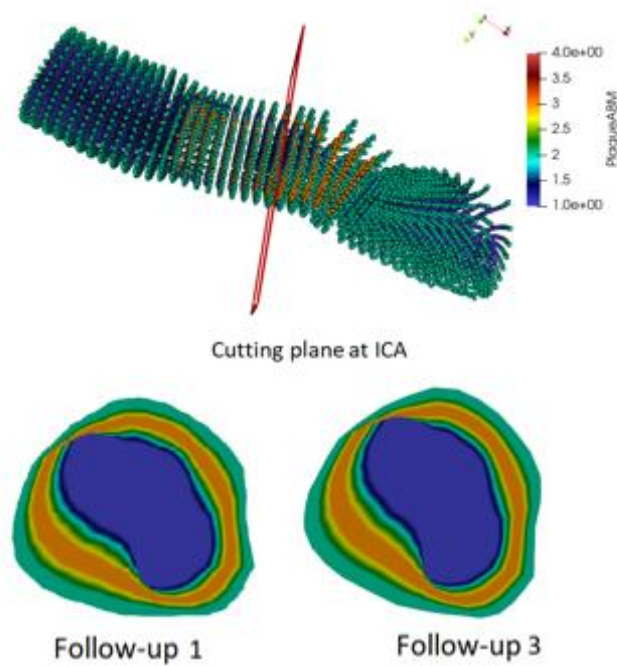


**Fig. 8.** Patient NKUA#4, follow-up 1 and follow-up 3 plaque results obtained with PAK ABM

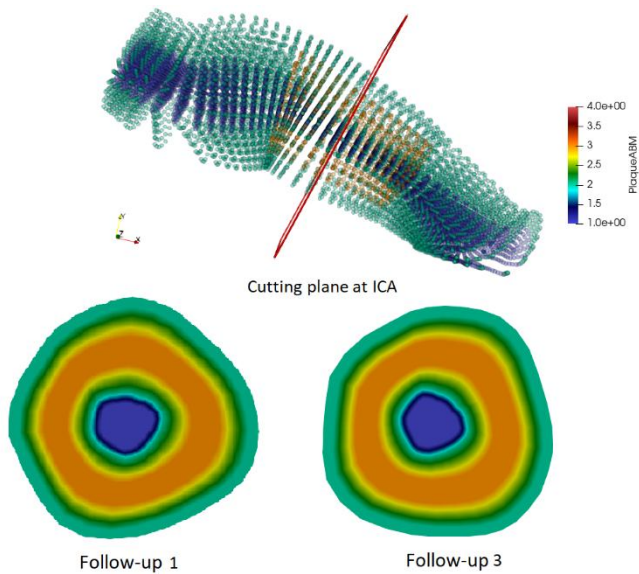


**Fig. 9.** Patient NKUA#6, follow-up 1 and follow-up 3 plaque results obtained with PAK ABM

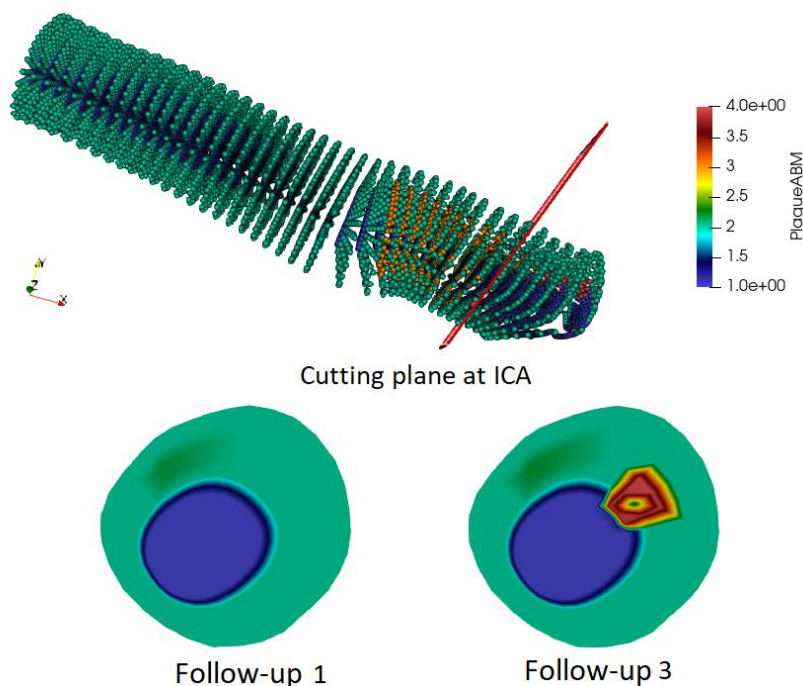


**Fig. 10.** Patient NKUA#25, follow-up 1 and follow-up 3 plaque results obtained with PAK ABM

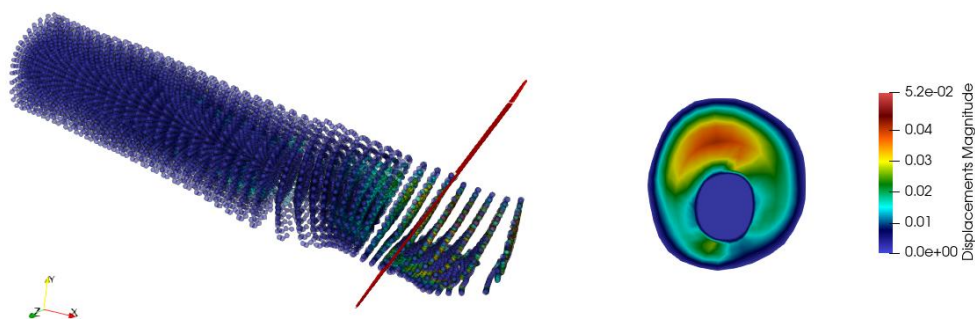


**Fig. 11.** Patient NKUA#25, displacements obtained with PAK ABM

#### 4. Discussion and conclusion

The ARTREAT project developed a detailed three-dimensional model for plaque formation and early progression, integrating blood flow dynamics and LDL concentration in the bloodstream. This model combines the Navier-Stokes equations with Darcy's law for blood filtration and Kedem-Katchalsky equations for solute and flux exchange, along with a system of three reaction-diffusion equations to simulate inflammation, all within an iterative incremental procedure. Wall permeability is modeled as a function of wall shear stress (WSS), increasing in regions of low and oscillatory shear stress. A patient-specific study identified three plaque



locations associated with low shear stress, and follow-up data showed close agreement between the simulated and measured plaque sizes. This computational approach provided valuable insights into plaque structure, representing a novel method for modeling plaque initiation and development (Filipovic et al., 2022). The correlation between plaque locations and progression over time highlights the potential of computer simulations to predict future vascular disease development.

Enhancing this framework, the Agent-Based Modeling and Simulation (ABMS) further improves the prediction of plaque growth in carotid arteries. ABM captures the evolution of plaque and arterial remodeling by simulating individual cellular agents. The coupling of finite element modeling (FEM) with ABM in patient-specific arterial models involves solving fluid dynamics equations, LDL transport, and fluid-structure interaction with mesh movement. This integrated approach has been validated against clinical data to ensure accuracy. In each time step, parameters such as blood velocity, LDL concentration, pressure, and shear stress are transferred from the FEM model to the ABM of the arterial wall. A fluid-structure solver updates the lumen domain accordingly, with the PAK-ABM simulator modeling the growth of plaques composed of lipid (soft), fibrous, and calcified (hard) materials. Different colors are used to represent these materials, as well as the wall and lumen, allowing users to customize visualizations during post-processing with Paraview on the Cloud TAXINOMISIS platform. Results from carotid artery simulations on this platform demonstrate that the findings are consistent with clinical observations (Filipovic et al., 2022; Filipovic, 2024).

## Acknowledgements

This review was funded by grants from EC: FP7-ICT-2007 224297 ARTREAT, and grants from Serbian Ministry of Science and Technological Development, EC grant: TAXINOMISIS European Union's Horizon 2020 Research and Innovation Programme under grant agreement No 755320.

## References

- ARTREAT project (2008-2013). *Multi-level patient-specific artery and atherogenesis model for outcome prediction, decision support treatment, and virtual hand-on training*, [www.artreat.org](http://www.artreat.org), [www.artreat.kg.ac.rs](http://www.artreat.kg.ac.rs)
- Bentzon, J F, Otsuka, F, Virmani, R, and Falk, E (2014). Mechanisms of plaque formation and rupture. *Circulation research*, 114(12), 1852-1866.
- Chan, S (2001). Complex Adaptive Systems. Research Seminar in Engineering Systems.
- Chatzizisis, Y, Coskun, A U, Jonas, M, Edelman, E, Feldman, C, & Stone, P (2007). Role of endothelial shear stress in the natural history of coronary atherosclerosis and vascular remodeling: molecular, cellular, and vascular behavior. *Journal of the American College of Cardiology*, 49(25), 2379-2393.
- Corti, A, Chiastra, C, Colombo, M, Garbey, M, Migliavacca, F, & Casarin, S (2020). A fully coupled computational fluid dynamics--agent-based model of atherosclerotic plaque development: multiscale modeling framework and parameter sensitivity analysis. *Computers in Biology and Medicine*, 118, 103623.
- Doran, A, Meller, N, & McNamara, C (2008). Role of smooth muscle cells in the initiation and early progression of atherosclerosis. *Arteriosclerosis, thrombosis, and vascular biology*, 28(5), 812-819.

- Filipovic, N, Teng Z, Radovic M, Saveljic I, Fotiadis D and Parodi O (2013). Computer simulation of three dimensional plaque formation and progression in the carotid artery, *Medical & Biological Engineering & Computing*, DOI: 10.1007/s11517-012-1031-4.
- Filipovic N, Rosic M, Tanaskovic I, Milosevic Z, Nikolic D, Zdravkovic N, Peulic A, Fotiadis D, Parodi O (2012). ARTreat project: Three-dimensional Numerical Simulation of Plaque Formation and Development in the Arteries, *IEEE Trans Inf Technol Biomed* 2012;16(2):272-278.
- Filipovic, N (2024). *In Silico Clinical Trials for Cardiovascular Disease: A Finite Element and Machine Learning Approach*, Springer 2024.
- Filipovic, N, Kojic, M, Slavkovic, R, Grujovic, N, & Zivkovic, M (2022) *PAK Athero, Finite element program for atherosclerosis*. BIOIRC doo Kragujevac, Serbia.
- Filipovic, N, Mijailovic, S, Tsuda, A, & Kojic, M (2006). An implicit algorithm within the arbitrary Lagrangian--Eulerian formulation for solving incompressible fluid flow with large boundary motions. *Computer methods in applied mechanics and engineering*, 195(44-47), 6347-6361.
- Garbey, M, Casarin, S, & Berceci, S (2017). Vascular adaptation: pattern formation and cross validation between an agent based model and a dynamical system. *Journal of theoretical biology*, 429, 149-163.
- Kaazempur-Mofrad MR, Ethier CR (2001). Mass transport in an anatomically realistic human right coronary artery, *Ann Biomed Eng* 2001;29:121–127.
- Kedem O, Katchalsky A (1958). Thermodynamic analysis of the permeability of biological membranes to non-electrolytes. *Biochim. Biophys* 1958; 27: 229–246.
- Kedem O, Katchalsky A (1961). A physical interpretation of the phenomenological coefficients of membrane permeability. *The Journal of General Physiology* 1961; 45: 143–179.
- Kojic, M, Filipovic, N, Stojanovic, B, & Kojic, N (2008). *Computer modeling in bioengineering: Theoretical Background, Examples and Software*. Chichester, England: John Wiley and Sons.
- Kojic, M, Filipovic, N, Živkovic, M, Slavkovic, R, & Grujovic, N (1998). *PAK-F Finite Element Program for Laminar Flow of Incompressible Fluid and Heat Transfer*. Kragujevac, Serbia.
- Otsuka, F, Nakano, M, Sakakura, K, Ladich, E, Kolodgie, F and Virmani, R (2013). Unique demands of the femoral anatomy and pathology and the need for unique interventions. *The Journal of Cardiovascular Surgery*, 54(2), 91-210.
- Samady, H, Eshtehardi, P, McDaniel, M C, Suo, J, Dhawan, S S, Maynard, C, Timmins, L H, Quyyumi, A, Giddens, D P (2011). Coronary artery wall shear stress is associated with progression and transformation of atherosclerotic plaque and arterial remodeling in patients with coronary artery disease. *Circulation*, 124(7), 779-788.
- TAXINOMISIS project (2018-2024). *A multidisciplinary approach for the stratification of patients with carotid artery disease*, <https://taxinomisis-project.eu/>